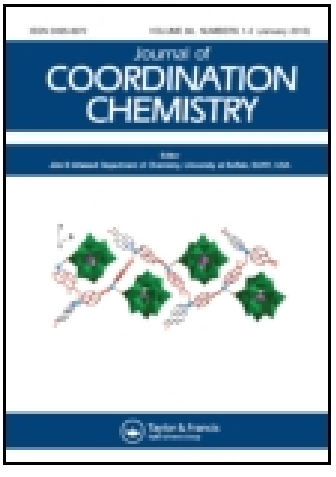



Journal of Coordination Chemistry
Publication details, including instructions for authors and subscription information:
http://www.tandfonline.com/loi/gcoo20

# An integrated experimental and theoretical investigation of the structural and spectroscopic properties of two nickel(II) isothiosemicarbazone complexes

Reza Takjoo[a], Ponnadurai Ramasami[b], Alireza Hashemzadeh[a], Lydia Rhyman[b], Hadi Amiri Rudbari[c] & Giuseppe Bruno[d]

[a] Department of Chemistry, School of Sciences, Ferdowsi University of Mashhad, Mashhad, Iran

[b] Computational Chemistry Group, Department of Chemistry, Faculty of Science, University of Mauritius, Réduit, Mauritius

[c] Faculty of Chemistry, University of Isfahan, Isfahan, Iran

[d] Dipartimento di Scienze Chimiche, Università di Messina, Messina, Italy

Accepted author version posted online: 22 Apr 2014.Published online: 05 Jun 2014.

To cite this article: Reza Takjoo, Ponnadurai Ramasami, Alireza Hashemzadeh, Lydia Rhyman, Hadi Amiri Rudbari & Giuseppe Bruno (2014) An integrated experimental and theoretical investigation of the structural and spectroscopic properties of two nickel(II) isothiosemicarbazone complexes, Journal of Coordination Chemistry, 67:8, 1392-1404, DOI: 10.1080/00958972.2014.916796

To link to this article: http://dx.doi.org/10.1080/00958972.2014.916796

*Journal of Coordination Chemistry*, 2014
Vol. 67, No. 8, 1392–1404, http://dx.doi.org/10.1080/00958972.2014.916796





# An integrated experimental and theoretical investigation of the structural and spectroscopic properties of two nickel(II) isothiosemicarbazone complexes

REZA TAKJOO*†, PONNADURAI RAMASAMI*‡, ALIREZA HASHEMZADEH†, LYDIA RHYMAN‡, HADI AMIRI RUDBARI§ and GIUSEPPE BRUNO¶

†Department of Chemistry, School of Sciences, Ferdowsi University of Mashhad, Mashhad, Iran
‡Computational Chemistry Group, Department of Chemistry, Faculty of Science, University of Mauritius, Réduit, Mauritius
§Faculty of Chemistry, University of Isfahan, Isfahan, Iran
¶Dipartimento di Scienze Chimiche, Università di Messina, Messina, Italy

(*Received 11 August 2013; accepted 25 March 2014*)

Allyl [(5-bromo-2-hydroxyphenyl) methylene]hydazincarboximidothioato (-2)-N,N2,O2](imidazole)nickel

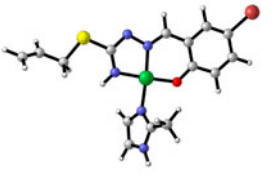

[Allyl [(5-bromo-2-hydroxyphenyl) methylene]hydazincarboximidothioato (-2)-N,N2,O2](2-methylimidazole)nickel

Two nickel(II) isothiosemicarbazone complexes of dianionic 5-bromosalicylaldehyde *S*-allyl isothiosemicarbazonehydrobromide ($H_2$L.HBr), [Ni(Im)L] and [Ni(2-MeIm)L] (Im: imidazole, 2-MeIm: 2-methylimidazole), were synthesized and characterized by single crystal X-ray crystallography, $^1$H NMR spectrometry, IR, and electronic spectroscopy. The complexes have square-planar geometry and the ligand is coordinated as a dinegative tridentate chelating agent via phenolic oxygen, isothioamide nitrogen, and azomethine nitrogen atoms. To complement the experimental data, density functional theory (DFT) and time-dependent DFT methods were used to validate the structural parameters and infrared and electronic spectra.

*Keywords*: Isothiosemicarbazone; Nickel(II) complex; Crystal structure; DFT; TDDFT

## 1. Introduction

The synthesis of isothiosemicarbazone led to studies involving its complexes [1–8]. Isothiosemicarbazide Schiff bases can exhibit different modes and charge due to the presence of $NH_2$ [1, 2]. Sulfur alkylation of thiosemicarbazone increases the coordinating ability of N

*Corresponding authors. Email: r.takjoo@um.ac.ir (R. Takjoo); ramchemi@intnet.mu (P. Ramasami)

(4) of the ligand [3, 9]. Homo and heterometallic complexes were synthesized [4–6] and these complexes have tunable steric [7] and electronic properties [8]. They are also soluble in many solvents and have interesting physical and chemical properties. It is reported that the presence of a lone pair [10] and the inclusion of bulky groups [11] on nitrogen atom of isothiosemicarbazone enhance the biological activity.

The Ni(II) square-planar Schiff base complexes have redox potentials of the $Ni^{I}/Ni^{II}$ and $Ni^{II}/Ni^{III}$ couples which enable them to be effective in many catalytic and biological reactions [12]. The lack of water solubility of these types of complexes makes them good candidates as heterogeneous catalysts [13]. In view of the interesting physicochemical properties, predicted bioinorganic chemistry, redox enzyme systems nuclease-like activity, DNA cleavage, and catalysis such as epoxidation of the C=C bond for isothiosemicarbazone complexes, more investigations are needed at molecular level for these complexes.

Theoretical methods have played an important role in gaining better insight into the bonding properties of complexes and in estimating the stability constants of the metal–ligand systems [14–17]. Density functional theory (DFT) is the most popular method used to support experimental data, namely X-ray crystallography and spectroscopic data [18–21]. For instance, Rulíšek and Havlas [22] reported that the B3LYP/6-311+G(d,p) method is computationally efficient for prediction of the molecular geometries and reaction energies of complexes. In 2010, Ahmedova and coworkers [23] carried out a combined experimental and theoretical study on nickel complexes of cyclohexanespiro-5-(2,4-dithiohydantoin). Due to the unavailability of crystallographic data of the resulting complex, they used the experimentally observed $^{13}C$ CPMAS NMR to determine the possible structures which were further supported by DFT computations, employing the B3LYP functional and the 6-31G(d,p) basis set. Several groups also characterized nickel complexes whereby the experimental findings were accurately reproduced by the DFT method [15, 16, 20, 23–29]. Atomic charge distribution, molecular electrostatic potential, and frontier molecular orbitals were also determined. These studies were extended by assessing the effect of changing solvents of the reactions and by analyzing the variation in the thermodynamic parameters at different temperatures.

Two mixed ligand isothiosemicarbazone Ni(II) complexes, **1** and **2**, [figures 1(a) and 1 (b)] were synthesized and characterized using X-ray and spectroscopic methods. This investigation was complemented using DFT and time-dependent DFT methods for simulating the electronic spectra.



## 2. Experimental

### 2.1. *Reagents and physical measurements*

All reagents used in the syntheses were commercially available and used without purification. 5-Bromosalicylaldehyde *S*-allyl isothiosemicarbazonehydrobromide was prepared as previously described [9].

Melting points were determined with a Barnstead Electrothermal 9200 apparatus. Conductivity was measured with a Herisau Metrohm CH-9101 apparatus using $10^{-3}$ M DMF solutions. Elemental analyses were performed on a Thermo Finnigan Flash Elemental Analyzer, model 1112EA. Infrared spectra of the complexes were recorded in KBr pellets with a FT-IR 8400-SHIMADZU spectrophotometer from 4000 to 400 $cm^{-1}$. Electronic

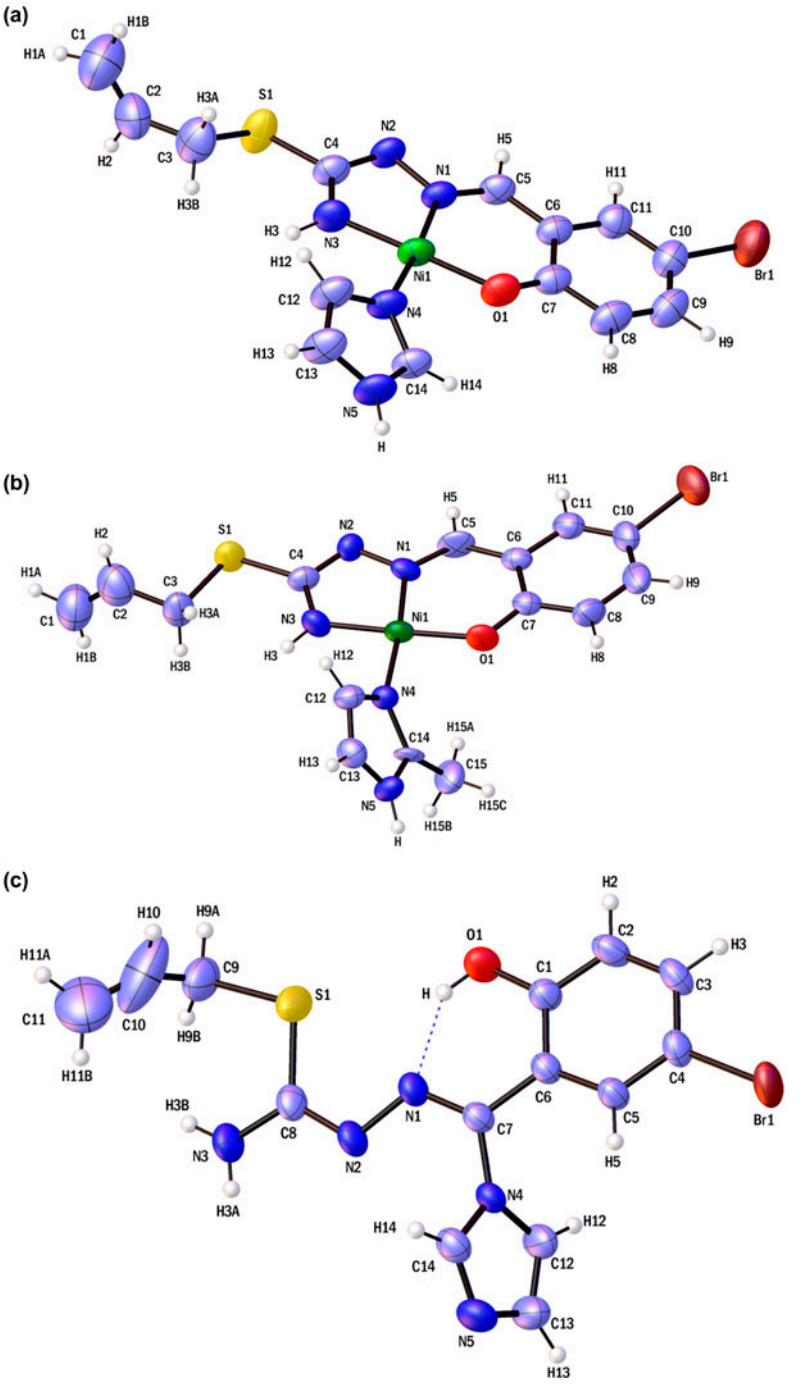


Figure 1. The crystal structure of **1** showing the atom numbering scheme. (a) Only one position is shown for the disordered *S*-allyl tail. (Displacement ellipsoids are drawn at the 50% probability level and hydrogens are shown as small spheres of arbitrary radii). (b) Perspective view and labeling of one of the two independent crystallographic units in **2**. (Displacement ellipsoids are drawn at the 50% probability level and hydrogens are shown as small spheres of arbitrary radii). (c) The crystal structure of **3** showing intermolecular hydrogen bonding.

absorption spectra were recorded using a SHIMADZU model 2550 UV–Vis spectrophotometer in methanol. The $^1$H NMR spectra were recorded in DMSO-$d_6$ and DMSO with a Bruker BRX 100 AVANCE spectrometer. Diffraction data were measured using a Bruker APEX II CCD area-detector diffractometer.

### 2.2. *General method of preparation*

$Ni(OAc)_2{\cdot}4H_2O$ (1.0 mM, 0.248 g) was added to an ethanolic solution of 5-bromosalicylaldehyde *S*-allyl isothiosemicarbazonehydrobromide (1 mM, 0.395 g) and appropriate amine (imidazole (2 mM, 0.136 g) for **1** and 2-methylimidazole (2 mM, 0.164 g) for **2**). The mixture was refluxed for 1 h at 80 °C. The resulting clear red solution was left to stand at room temperature. After a few days, crystalline complexes were obtained. The product was filtered off, washed with cold ethanol, and dried over anhydrous silica gel in a desiccator.

Note: For preparation of **1**, triethylamine (2 mM, 0.022 g) was added to the mixture.

**2.2.1. 5-Bromosalicylaldehyde *S*-allyl isothiosemicarbazonato(2-)imidazolenickel(II) (1).** [Ni(Im)L]: Irregular, red. Yield: 0.290 g, 66%. M.p.: 211.9 °C. Molar conductivity: 6 $\Omega^{-1}\,cm^{-2}\,M^{-1}$. Anal. Calcd for $C_{14}H_{14}BrN_5NiOS$ (438.96 g $M^{-1}$): C, 38.31; H, 3.21; N, 15.95; S, 7.30. Found: C, 36.44; H, 3.13; N, 16.97; S, 6.86%. IR (KBr) $cm^{-1}$: $\nu$(NH) 3411s, $\nu$(C=N) 1591m, 1623-m, $\nu$(C=C) 1458m, $\nu$(C=N) 1507s, $\nu$(Im) 1225w, $\nu$(C–O) 1185w, $\nu$(N–N) 1066m. UV/Vis (methanol) $\lambda_{max}$, nm (log$\varepsilon$, L $M^{-1}$ $cm^{-1}$): 220 (4.78), 248 (4.63), 304 (4.37), 380 (4.23). $^1$H NMR (100 MHz, DMSO-$d_6$): $\delta$ = 12.8 (s, 1H, N5H), 8.0 (s, 2H, C5H5, C14H14), 7.6 (d, 1H, C11H11), 7.2 (m, 3H, C9H9, C12H12, C13H13), 6.7 (d, 1H, C8H8), 5.8 (s, 1H, C2H2), 5.2 (m, 2H, C1H1), 4.2 (s, 1H, N3H), 3.7 (d, 1H, C3H3).

**2.2.2. 5-Bromosalicylaldehyde *S*-allyl isothiosemicarbazonato(2-)2-methylimidazolenickel(II) (2).** [Ni(2-MeIm)L]: Irregular, red. Yield: 0.229 g, 66.1%. M.p.: 193.1 °C. Molar conductivity: 8 $\Omega^{-1}\,cm^{-2}\,M^{-1}$. Anal. Calcd for $C_{15}H_{16}BrN_5NiOS$ (452.98 g $M^{-1}$): C, 39.77; H, 3.56; N, 15.46; S, 7.08. Found: C, 38.02; H, 3.26; N, 15.71; S, 6.31%. IR (KBr) $cm^{-1}$: $\nu$(NH) 3425s, 3467; $\nu$(C=N) 1621w, 1583m, 1496s; $\nu$(C=C) 1420w; $\nu$(C–O) 1237m; $\nu$(N–N) 1123w. UV/Vis (methanol) $\lambda_{max}$, nm (log$\varepsilon$, L $M^{-1}$ $cm^{-1}$): 222 (3.15), 248 (4.45), 306 (4.49), 376 (4.45), 590 (3.15). $^1$H NMR (100 MHz, DMSO-$d_6$): $\delta$ = 12.5 (s, 1H, N5H), 8.1 (s, 1H, C5H5), 7.6 (d, 1H, C11H11), 7.2 (m, 3H, C9H9, C12H12, C13H13), 6.6 (d, 1H, C8H8), 5.9 (s, 1H, C2H2), 5.2 (m, 2H, C1H1), 4.2 (d, 1H, N3H), 3.7 (d, 2H, C3H3), 3.2 (d, 1H, CHIm), 2.8 (s, 3H, C15H15).

### 2.3. *Structure determination*

Single-crystal X-ray diffraction data for **1–3** [figures 1(a)–1(c)] were collected on a Bruker APEX II equipped with a CCD area detector and utilizing Mo-$K_\alpha$ radiation ($\lambda$ = 0.71073 Å) at room temperature. Data were collected and reduced by SMART and SAINT software in the Bruker packages [30]. The structures were solved by direct methods [31] [SHELXTL.97] and then solved by least-squares refinement on $F^2$ [32, 33]. The complete conditions of data collection and structure refinements parameters are given in table 1. All hydrogens were placed in calculated positions and refined as isotropic with the "riding-model technique".

### 2.4. *Computational methods*

The structures of the nickel(II) complexes in the ground state were optimized in the gas phase using the DFT method. Several standard functionals, B3LYP, BH, HLYP, BLYP, PBE1PBE and X3LYP were used. In all computations, the LANL2DZ basis set was used for nickel and the 6-311+G(d,p) basis set was used for carbon, nitrogen, oxygen, and sulfur atoms. Frequency computation of the optimized geometry was performed to ensure that the complex was a true local minimum. Uncorrected infrared vibrational frequencies and HOMO–LUMO gap of the two complexes are reported for the B3LYP functional. TDDFT computations were carried out using the optimized structures in methanol to obtain the electronic spectra.

In DFT framework [34], two parameters $\mu$ and $\eta$ were calculated using HOMO and LUMO energies as:

$$\mu \cong \frac{1}{2}(E_{\mathrm{LUMO}} + E_{\mathrm{HOMO}}) \tag{1}$$

Table 1. Crystal data and structure refinements parameters for **1–3**.

| Empirical formula | $C_{14}H_{14}BrN_5NiOS$ (**1**) | $C_{15}H_{16}BrN_5NiOS$ (**2**) | $C_{14}H_{14}BrN_5OS$ (**3**) |
|---|---|---|---|
| Formula weight | 438.98 | 453.01 | 380.27 |
| Temperature (K) | 298(2) | 298(2) | 298(2) |
| Wavelength (Å) | 0.71073 | 0.71073 | 0.71073 |
| Crystal system, space group | Triclinic, $P\bar{1}$ | Monoclinic, $P2_1/c$ | Monoclinic, $C2/c$ |
| Unit cell dimensions | $a$ = 8.0642(2) Å<br>$b$ = 9.2143(2) Å<br>$c$ = 13.0313(3) Å<br>$\alpha$ = 73.9146(9)°<br>$\beta$ = 86.7943(9)°<br>$\gamma$ = 65.5459(8)° | $a$ = 26.1862(8) Å<br>$b$ = 7.7684(2) Å<br>$c$ = 18.2586(6) Å<br>$\beta$ = 110.0680(10)° | $a$ = 30.4985(14) Å<br>$b$ = 5.2727(2) Å<br>$c$ = 23.2595(11) Å<br>$\beta$ = 120.750(3)° |
| Volume ($A^3$) | 845.02(3) | 3488.75(18) | 3214.5(2) |
| $Z$, calculated density (mg $m^{-3}$) | 2, 1.725 | 8, 1.725 | 8, 1.572 |
| Absorption coefficient ($mm^{-1}$) | 3.645 | 3.535 | 2.696 |
| $F$ (0 0 0) | 440 | 1824 | 1536 |
| Crystal size (mm) | 0.23 × 0.21 × 0.12 | 0.17 × 0.16 × 0.12 | 0.23 × 0.18 × 0.16 |
| $\theta$ Range for data collection | 2.78–27.00° | 0.83–25.00° | 1.55–25.00° |
| Limiting indices | $-10 \le h \le 10$, $-11 \le k \le 11$, $-16 \le l \le 16$ | $-31 \le h \le 31$, $-9 \le k \le 9$, $-21 \le l \le 21$ | $-36 \le h \le 36$, $-6 \le k \le 6$, $-27 \le l \le 27$ |
| Reflections collected/ unique | 18,142/3664 [$R_{(int)}$ = 0.0249] | 98,704/6146 [$R_{(int)}$ = 0.0405] | 42,745/2837 [$R_{(int)}$ = 0.0394] |
| Completeness to $\theta$ = 26.00 | 99.50% | 99.80% | 99.90% |
| Refinement method | Full-matrix least-squares on $F^2$ | Full-matrix least-squares on $F^2$ | Full-matrix least-squares on $F^2$ |
| Data/restraints/ parameters | 3664/2/226 | 6146/0/433 | 2837/2/221 |
| Goodness-of-fit on $F^2$ | 1.043 | 1.103 | 1.092 |
| Final $R$ indices [$I > 2\sigma(I)$] | $R_1$ = 0.0291, $wR_2$ = 0.0746 | $R_1$ = 0.0824, $wR_2$ = 0.1532 | $R_1$ = 0.0368, $wR_2$ = 0.1081 |
| $R$ indices (all data) | $R_1$ = 0.0372, $wR_2$ = 0.0791 | $R_1$ = 0.1127, $wR_2$ = 0.1901 | $R_1$ = 0.0481, $wR_2$ = 0.1334 |
| Largest diff. peak and hole (e $A^{-3}$) | 0.727 and −0.615 | 2.166 and −1.355 | 0.863 and −0.630 |

$$\eta \cong \frac{1}{2}(E_{\mathrm{LUMO}} - E_{\mathrm{HOMO}}) \quad (2)$$

Gaussian 09 program was used for all the computations [35].

## 3. Results and discussion

Complexes **1** and **2** were obtained from reaction of 5-bromosalicylaldehyde *S*-allyl isothiosemicarbazonehydrobromide, $Ni(OAc)_2{\cdot}4H_2O$ and imidazole (for **1**) or 2-methylimidazole (for **2**) with 1 : 1 : 2 M ratio in ethanolic solution. The analytical data of the products are in agreement with their respective formulas. Molar conductivity values of the complexes are in accord with their non-electrolytic nature. X-ray crystallography was used to determine the structures of all crystals.

Similar reactions were performed with manganese(II) instead of nickel(II) and in all cases, no precipitate was observed. The slow evaporation of the filtrate resulted in an unknown precipitate and a few small poorly shaped crystals. Recrystallization of this filtrate led to some pale yellow crystals. The allyl ((5-bromo-2-hydroxyphenyl)(1H-imidazole-1-yl) methylene)hydrazinecarboximidothioate (**3**) structure was determined for these crystals by X-ray crystallography.

### 3.1. *Characterization of the complex species*

**3.1.1. IR spectra of the complexes.** In comparison to the solid state IR spectrum of the ligand [9] and the complexes, the $\nu$(OH) band of the ligand at 3173 $cm^{-1}$ does not appear in the spectra of the complexes and indicates that the ligand coordinated to nickel is in its deprotonated form [36]. In this section, the data within brackets correspond to the uncorrected frequencies predicted at the B3LYP level of theory in the gas phase. The experimental IR spectra of the complexes are illustrated in figures SI 1(a) and SI 1(b). The simulated IR spectra in the gas phase for the complexes are collected in figures SI 2(a) and SI 2(b). Both **1** and **2** display two bands at 3414 (3603) and 3425 (3620) $cm^{-1}$ which are attributed to $\nu$(N–H) of isothioamide [7]. The bands at 1509 (1558), 1590 (1562), and 1624 (1653) $cm^{-1}$ for **1** and 1496 (1552), 1583 (1560), and 1621 (1650) $cm^{-1}$ for **2** are assigned to C=N bond stretching vibrations corresponding to the isothiosemicarbazone and imidazole (or 2-methylimidazole) moieties respectively. The $\nu$(C–O) stretch at 1185 (1344) and 1237 (1343) $cm^{-1}$ in the spectra of **1** and **2** respectively, supports the coordination of the phenolic oxygen atom to the metal atom [37]. The absorption appearing at 1066 (1073) and 1123 (1069) $cm^{-1}$ corresponds to the N–N stretch in **1** and **2** respectively.

**3.1.2. $^1$H NMR spectra of the complexes.** Experimental $^1$H NMR spectra of the two complexes are displayed in figures SI 3(a) and SI 3(b). In these, $^1$H NMR spectra of **1** and **2** in DMSO-$d_6$, signals appear at 12.8 and 12.5 ppm for the NH proton of imidazole and 2-methylimidazole respectively. These confirm the presence of an imidazole and 2-methylimidazole in the complexes. The spectra do not exhibit any signal attributable to the OH

proton which is expected at 11.4 and 10.8 ppm for the ligands. This indicates that the ligand is coordinated to the metal center via the deprotonated phenolic oxygen. After complex-formation, the azomethine proton in the ligand at 8.7 ppm is shifted upfield to 8.2 and 8.1 ppm and this suggests coordination via the azomethine nitrogen.

**3.1.3. Electronic spectra of the complexes.** The electronic spectra of the two complexes in methanol in the ultraviolet region are given in figures SI 4(a) and SI 4(b). The spectrum of **1** exhibits bands at 220 and 248 nm, attributed to $\pi \rightarrow \pi^*$ transitions of the ring and isothiosemicarbazone respectively. Similarly, $\pi \rightarrow \pi^*$ transitions are observed at 222 and 248 nm in **2**. In the complexes, the $\pi \rightarrow \pi^*$ transitions exhibited significant blue shift compared to the ligand (226 and 304 nm) and this indicates coordination of nitrogen and oxygen atoms to nickel ion. The bands at 304–306 and 376–380 nm are assigned to the $n \rightarrow \pi^*$ transitions and showed hypsochromic and bathochromic shift compared to the ligand $n \rightarrow \pi^*$ transitions (312 and 446 nm) respectively. Complex **1** did not exhibit a band in the visible region but a band was found at 590 nm in **2**. The three expected d–d transitions for square-planar nickel compounds were hidden by a strong LMCT transition [38]. The simulated electronic spectra (B3LYP) in methanol for **1** and **2** are shown in figures SI 5(a) and SI 5(b). These electronic spectra are characterized by three bands at 250–300, 330–360, and 370–400; details at the molecular level are available from table 2.

The frontier molecular orbitals (HOMO and LUMO) of **1** and **2** in methanol are illustrated in figure 2(a) and (b). The electron densities are delocalized over the complexes excluding the allyl and the imidazole or 2-methylimidazole moieties. The HOMO–LUMO gaps of **1** and **2** in methanol are 332 and 334 eV respectively. These gaps lead to $\mu$ and $\eta$ to be 180.50 and 178.99 kJ mol$^{-1}$, and −358.49 and −353.62 kJ mol$^{-1}$, correspondingly. These large gaps and derived parameters contribute to their stabilities which make them suitable for specific applications such as plastic colorant and drying agents [39].

### 3.2. *Description of the crystal structures*

The basic crystallographic data and characteristics of **1–3** are collected in table 1. The molecular structures of **1–3** with atom numbering schemes are shown in figures 1(a)–1(c) respectively. The dipole moments of **1** and **2** are 8.8 and 11.6 Debye, correspondingly. Selected geometrical parameters are presented in table 3 together with the predicted values using the different functionals. An analysis of the data in the table indicates a good comparison between the experimental and predicted parameters. To be more precise, for the

Table 2. Selected parameters of the electronic spectra of **1** and **2** in methanol.

| Wavelength (nm) | Oscillator strength | Main configuration |
|---|---|---|
| Complex **1** | | |
| 266.9 | 0.074 | HOMO ($\alpha$) → LUMO+3 ($\alpha$) |
| 290.5 | 0.106 | HOMO-2 ($\alpha$) → LUMO ($\alpha$) |
| 350.0 | 0.145 | HOMO-1 ($\alpha$) → LUMO ($\alpha$) |
| 380.5 | 0.357 | HOMO ($\alpha$) → LUMO ($\alpha$) |
| Complex **2** | | |
| 270.2 | 0.068 | HOMO ($\alpha$) → LUMO+4 ($\alpha$) |
| 288.6 | 0.108 | HOMO-3 ($\alpha$) → LUMO ($\alpha$) |
| 347.9 | 0.161 | HOMO-1 ($\alpha$) → LUMO ($\alpha$) |
| 383.2 | 0.437 | HOMO ($\alpha$) → LUMO ($\alpha$) |

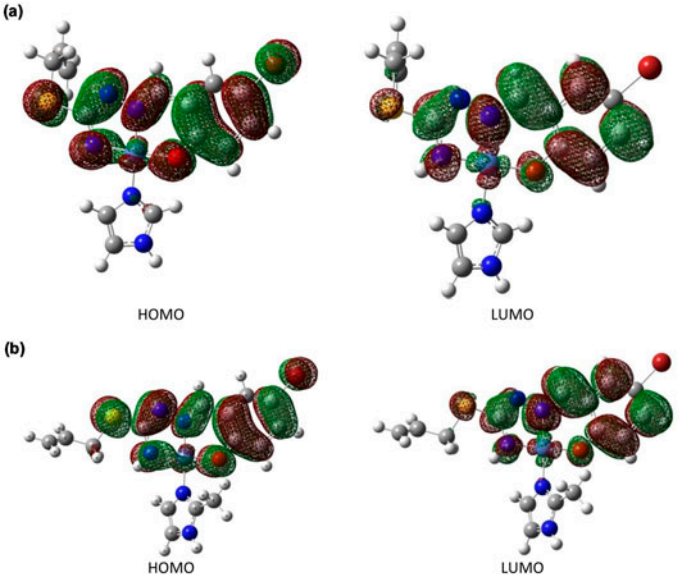


Figure 2. (a) Frontier molecular orbital of **1**. (b) Frontier molecular orbital of **2**.

different functionals, the standard deviations range from 0.015 to 0.045 Å and 0.9° to 1.4° for the selected bond lengths and bond angles respectively.

In both crystals, the isothiosemicarbazone shows an *E* configuration about the C4–N2–N1–C5 chain and this is conventional behavior in this type of compound [38, 40]. The $L^{2-}$ in the complexes is coordinated to nickel in its bi-deprotonated form via phenolic oxygen, isothioamide nitrogen and azomethine nitrogen atoms. This tridentate dianionic ONN donor is coordinated to nickel by forming stable five- and six-membered rings. The coordination around nickel(II) is distorted square planar in both complexes.

The crystal structure of **1** consists of one discrete molecular unit, while that of **2** consists of two molecular neutral units, Ni1 and Ni2 molecular units which are crystallographically independent, but chemically similar (see figure SI 6). A comparison of the N(1)–N(2) distance in **1** (1.398(2) Å) and **2** (1.39(2) Å) with other similar compounds [9, 38, 41] reveals that this bond is shorter than the expected value for a single N–N bond (1.44 Å). In addition, C5–N1 bond distance values of 1.286(3) and 1.28(2) Å in **1** and **2** respectively, are in agreement with the C=N expected bond length. This observation indicates delocalization of $\pi$-charge along the C4–N2–N1–C5 moiety [7]. The dihedral angle between imidazole and 2-methylimidazole mean plane with the mean plane of C4–N2–N1–C5 is 23.84° and 56.93° in **1** and **2** respectively. The maximum distortions from the ideal geometry around Ni occur for N1–Ni–O1 angle in these two complexes.

In **1**, a short intermolecular hydrogen bond involving imidazole N5 and hydrazinic N2 (N5–H···N2 (2.903(3) Å) leads to the formation of a 1-D supramolecular nickel complex with $C_1^1(7)$ graph set (figure 3) along the −110 direction. Hydrogen bonding causes more crystal growth along (0, 0, 1) and (0, 0, −1) planes. Weak intermolecular interaction of the type C1-H11A···C10 (3.762(7) Å) extended the chain in 1-D along the *c* axis. In **1**, the C2 of the allyl group is disordered over two positions.

Table 3. Selected bond lengths (Å) and angles (°) of **1** and **2**.

| | Expt. | B3LYP | BHLYP | BLYP | PBE1PBE | X3LYP |
|---|---|---|---|---|---|---|
| Complex **1** | | | | | | |
| Ni1–O1 | 1.8344(17) | 1.863 | 1.855 | 1.878 | 1.848 | 1.861 |
| Ni1–N3 | 1.840(2) | 1.874 | 1.876 | 1.888 | 1.855 | 1.872 |
| Ni1–N1 | 1.8477(17) | 1.873 | 1.884 | 1.878 | 1.857 | 1.873 |
| Ni1–N4 | 1.9025(17) | 1.954 | 1.903 | 1.969 | 1.931 | 1.952 |
| S(1)–C(4) | 1.756(2) | 1.784 | 1.769 | 1.801 | 1.768 | 1.782 |
| S(1)–C(3) | 1.804(3) | 1.835 | 1.814 | 1.860 | 1.814 | 1.833 |
| C(7)–O(1) | 1.304(3) | 1.311 | 1.298 | 1.326 | 1.303 | 1.310 |
| N(1)–C(5) | 1.286(3) | 1.302 | 1.281 | 1.322 | 1.297 | 1.300 |
| N(1)–N(2) | 1.398(2) | 1.385 | 1.377 | 1.397 | 1.372 | 1.384 |
| N(2)–C(4) | 1.311(3) | 1.316 | 1.301 | 1.330 | 1.311 | 1.315 |
| C(4)–N(3) | 1.321(3) | 1.341 | 1.330 | 1.354 | 1.335 | 1.340 |
| O(1)–Ni(1)–N(3) | 176.25(8) | 177.3 | 175.8 | 178.1 | 177.6 | 177.2 |
| O(1)–Ni(1)–N(1) | 95.45(8) | 95.4 | 94.5 | 96.0 | 95.8 | 95.4 |
| N(3)–Ni(1)–N(1) | 82.54(8) | 82.1 | 81.6 | 82.3 | 82.3 | 82.1 |
| O(1)–Ni(1)–N(4) | 88.99(8) | 88.1 | 88.4 | 88.0 | 87.9 | 88.1 |
| N(3)–Ni(1)–N(4) | 93.18(8) | 94.3 | 95.5 | 93.8 | 94.1 | 94.4 |
| N(1)–Ni(1)–N(4) | 174.65(8) | 176.1 | 176.6 | 175.9 | 176.0 | 176.1 |
| Complex **2** | | | | | | |
| Ni1–O1 | 1.828(11)/1.840(10) | 1.861 | 1.852 | 1.878 | 1.847 | 1.859 |
| Ni1–N3 | 1.842(13)/1.796(13) | 1.872 | 1.874 | 1.888 | 1.853 | 1.870 |
| Ni1–N1 | 1.850(11)/1.838(11) | 1.873 | 1.883 | 1.878 | 1.858 | 1.873 |
| Ni1–N4 | 1.912(11)/1.913(11) | 1.957 | 1.956 | 1.976 | 1.933 | 1.954 |
| S(1)–C(4) | 1.753(15)/1.767(16) | 1.783 | 1.770 | 1.799 | 1.768 | 1.782 |
| S(1)–C(3) | 1.808(17)/1.90(3) | 1.853 | 1.828 | 1.886 | 1.830 | 1.850 |
| C(7)–O(1) | 1.316(18)/1.302(18) | 1.311 | 1.298 | 1.326 | 1.303 | 1.310 |
| N(1)–C(5) | 1.28(2)/1.319(19) | 1.303 | 1.282 | 1.323 | 1.298 | 1.301 |
| N(1)–N(2) | 1.389(16)/1.424(18) | 1.384 | 1.376 | 1.396 | 1.371 | 1.383 |
| N(2)–C(4) | 1.339(19)/1.31(2) | 1.318 | 1.302 | 1.332 | 1.314 | 1.317 |
| C(4)–N(3) | 1.305(18)/1.330(18) | 1.343 | 1.331 | 1.356 | 1.337 | 1.342 |
| O(1)–Ni(1)–N(3) | 177.9(5)/177.3(5) | 177.5 | 176.3 | 177.6 | 178.0 | 177.5 |
| O(1)–Ni(1)–N(1) | 96.0(5)/95.5(5) | 95.5 | 94.5 | 96.0 | 95.8 | 95.4 |
| N(3)–Ni(1)–N(1) | 81.8(5)/83.0(5) | 82.3 | 81.8 | 82.4 | 82.4 | 82.3 |
| O(1)–Ni(1)–N(4) | 89.1(5)/89.5(5) | 89.3 | 90.1 | 88.9 | 89.2 | 89.4 |
| N(3)–Ni(1)–N(4) | 93.0(5)/92.2(5) | 93.0 | 93.6 | 92.7 | 92.6 | 92.9 |
| N(1)–Ni(1)–N(4) | 174.6(5)/174.2(6) | 175.2 | 175.2 | 175.1 | 175.0 | 175.2 |

In **2**, N2 and N7 are hydrogen bond acceptors and they form two $C_1^1(7)$ graph set. The N5–H···N2 (2.845(2) Å) and N10–H10···N7 (2.845(2) Å) hydrogen bonds develop two individual 1-D supramolecular chains along the *c* axis (figure 4). This collection extends to another dimension along the *c* axis by C15–H15B···O1 (3.386(3) Å) hydrogen bonding.

We have already prepared the Cu complex which is isostructural to **1** [9]. Comparison between these two compounds shows interesting cases: (1) they have two different space groups, (2) the imidazole ring has wrest around the C4–N2–N1–C5 mean plane about 23.84° and 9.97° in **1** and its isostructural Cu-complex respectively, (3) the allyl group is along the isothiosemicarbazone skeleton and parallel to imidazole in **1** and the Cu complex respectively, and (4) both Ni and Cu compounds have a $C_1^1(7)$ a graph set but **1** and the Cu complex show two different angles between the mean plane of the two adjacent molecules which are 0° and 74.18° respectively.

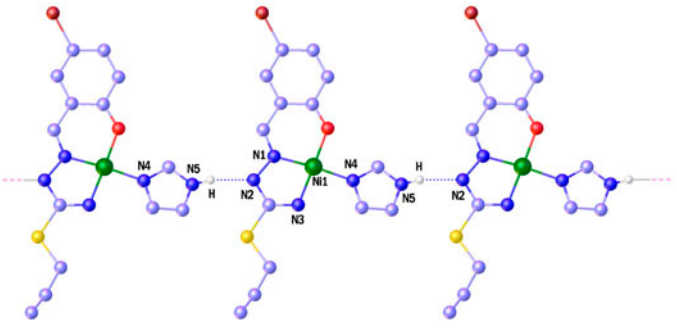


Figure 3. Fragment of molecules of **1** joining up along the −110 direction. Hydrogen bonds are indicated by dashed lines. Hydrogens have been omitted for clarity except hydrogens that participate in the hydrogen bonds.

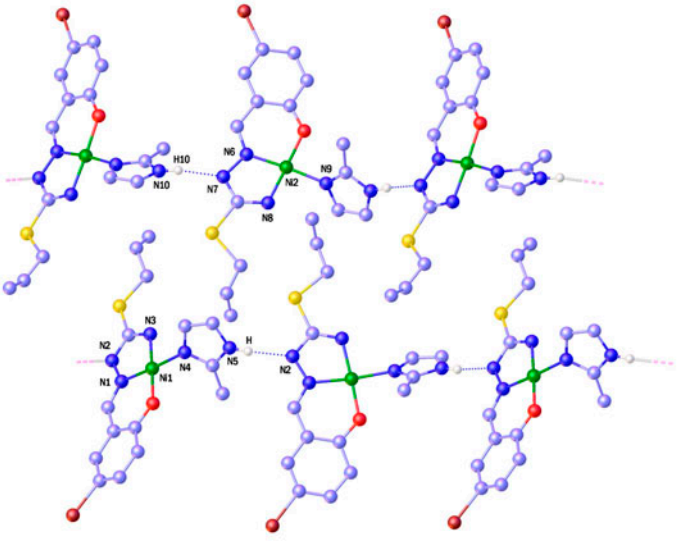


Figure 4. Extension of two individual $C_1^1(7)$ graph sets along the *c* axis in **2**. Hydrogen bonds are indicated by dashed lines. Hydrogens have been omitted for clarity except those that participate in hydrogen bonds.

In **3**, an intramolecular hydrogen bond forms between the hydrazinic nitrogen (N1) and the hydrogen of hydroxyl (O1···H) by 2.626(3) Å with $S_1^1(6)$ graph set [figure 1(c)]. Two intermolecular N3–H3A···N2 (3.066(5) Å) hydrogen bonds link two adjacent molecules as a dimer with $R_2^2(8)$ graph set (figure 5). The presence of a N3–H3B···N5 (2.983(4) Å) hydrogen bond causes the expansion of these dimers along the *a* axis with $C_1^1(9)$ graph set as a ribbon (figure 6). The Br1···Br1 interaction (2.8673(6) Å) along the *a* axis connects these ribbons and makes 2-D networks. The C2–H2···O1 hydrogen bond (3.343(5) Å) links the 2-D structure to form a 3-D network structure.

CSD studies show 21 square-planar structures of tridentate isothiosemicarbazone complexes and all of these compounds have nickel and copper as central ions (table SI1).

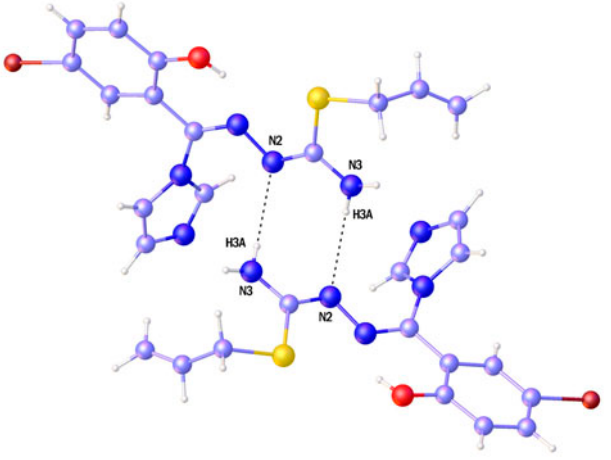


Figure 5. A dimer of **3**.

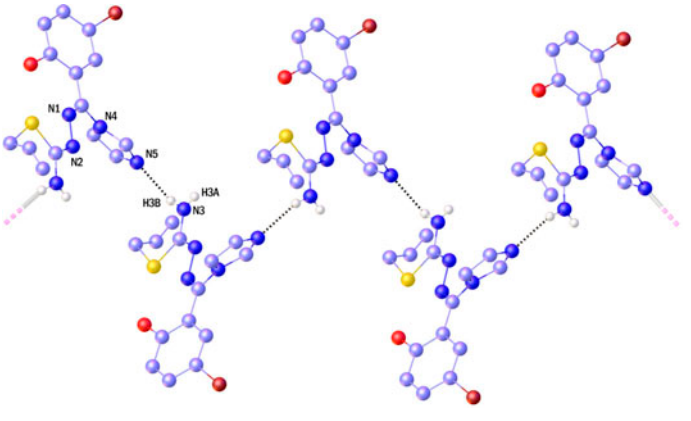


Figure 6. 1-D ribbon of **3** along the *a* axis. Hydrogens have been omitted for clarity except hydrogens that participate in intermolecular hydrogen bonds.

Among these compounds, the (*S*-methyl-N1-(salicylidene)-isothiosemicarbazidato)-pyridyl-nickel(II) perchlorate methanol solvate is the only one in which the $NH_2$ group is connected to Ni(II) without deprotonation and forms a cationic complex [42]. The positively charged metal center causes the shortest Ni–O (1.809(8) Å) and Ni–N3 (1.87(1) Å) and the longest Ni–N2 (1.88(1) Å) bond distances to be observed in these 21 square-planar compounds. Other nickel complexes are neutral and among them, **1** has the shortest Ni–N3 bond distance (1.902(2) Å). Since the methyl group of 2-methylimidazole causes a severe steric effect with the chelating ligand and causes high rotation of 2-methylimidazole by 56.93°, the biggest dihedral angle is observed in **2**. Regardless of **2**, the dihedral angle between pyridine and its derivative complexes is bigger than the imidazole analogous compounds.

## 4. Conclusions

Two Ni(II) complexes of isothiosemicarbazone were synthesized and characterized by various physicochemical analyses. The ligand is binegative NNO tridentate, coordinating through phenolic oxygen, azomethine and isothioamide nitrogens atoms. The physical data and X-ray crystallography support square-planar geometry for both complexes. DFT- and TD DFT-based computations were used for validating the structural and spectroscopic parameters of the complexes. The findings from this research should be helpful towards the applications and use of these polar complexes.



## Supplementary material

Supplementary data CCDC 943807–943809 contain the supplementary crystallographic data for the compounds. These data can be obtained free of charge via http://www.ccdc.cam.ac.uk/conts/retrieving.html, or from the Cambridge Crystallographic Data Center, 12 Union Road, Cambridge CB2 1EZ, UK; Fax: (+44) 1223-336-033; or E-mail: deposit@ccdc.cam.ac.uk.

## Acknowledgements

The authors acknowledge facilities from the Ferdowsi University of Mashhad, University of Mauritius, University of Isfahan and Università degli Studi di Messina. We also acknowledge the useful comments from the reviewers to improve the manuscript.

## Supplemental data

Supplemental data for this article can be accessed here. [http://dx.doi.org/10.1080/00958972.2014.916796].

## References

[1] Ş. Güveli, B. Ülküseven. *Polyhedron*, **30**, 1385 (2011).
[2] Y. Gao, L. Zhao, X. Xu, G.F. Xu, Y.N. Guo, J. Tang, Z. Liu. *Inorg. Chem.*, **50**, 1304 (2011).
[3] S.B. Novaković, G.A. Bogdanović, V.M. Leovac. *Polyhedron*, **25**, 1096 (2006).
[4] F.K. Zhovmir, Yu.A. Simonov, V.V. Zelentsov, N.V. Gerbeleu, M.D. Revenko, A.K. Stroesku, A.N. Sobolev. *Zh. Neorg. Khim.*, **33**, 2180 (1988).
[5] V.M. Leovac, V.I. Češljević, L.S. Vojinović-Ješić, V. Divjaković, L.S. Jovanović, K.M. Szécsényi, M.V. Rodić. *Polyhedron*, **28**, 3570 (2009).
[6] J.-P. Costes, F. Dahan, G. Novitchi, V. Arion, S. Shova, J. Lipkowski. *Eur. J. Inorg. Chem.*, **2004,** 1530 (2004).
[7] M.V. Rodić, V.M. Leovac, L.S. Jovanović, L.S. Vojinović-Ješić, V. Divjaković, V.I. Češljević. *Polyhedron*, **46**, 124 (2012).
[8] V. Leovac, V. Divjakovic, M. Joksovic, L. Jovanovic, L. Vojinovic-Jesic, V. Cesljevic, M. Mlinar. *J. Serb. Chem. Soc.*, **75**, 1063 (2010).
[9] R. Takjoo, A. Hashemzadeh, H.A. Rudbari, F. Nicolo. *J. Coord. Chem.*, **66**, 345 (2013).
[10] M. Shakir, M. Azam, M.F. Ullah, S.M. Hadi. *J. Photochem. Photobiol., B*, **104**, 449 (2011).
[11] R.R. Zaky. *Phosphorus, Sulfur Silicon Relat. Elem.*, **186**, 365 (2011).

[12] R.M. El-Shazly, G.A. Al-Hazmi, S.E. Ghazy, M.S. El-Shahawi, A.A. El-Asmy. *Spectrochim. Acta A Mol. Biomol. Spectrosc.*, **61**, 243 (2005).
[13] H. Eshtiagh-Hosseini, T. Tabari, R. Takjoo, H. Eshghi. *Synth. React. Inorg. Met.-Org. Nano-Met. Chem.*, **43**, 264 (2013).
[14] M.T. Kieber-Emmons, J. Annaraj, M.S. Seo, K.M. Van Heuvelen, T. Tosha, T. Kitagawa, T.C. Brunold, W. Nam, C.G. Riordan. *J. Am. Chem. Soc.*, **128**, 14230 (2006).
[15] J. Cho, R. Sarangi, J. Annaraj, S.Y. Kim, M. Kubo, T. Ogura, E.I. Solomon, W. Nam. *Nat. Chem.*, **1**, 568 (2009).
[16] A. Wojciechowska, M. Daszkiewicz, Z. Staszak, A. Trusz-Zdybek, A. Bieńko, A. Ozarowski. *Inorg. Chem.*, **50**, 11532 (2011).
[17] D. Chopra. *J. Phys. Chem. A*, **116**, 9791 (2012).
[18] A. Ricca, C.W. Bauschlicher Jr. *J. Phys. Chem.*, **99**, 9003 (1995).
[19] A.P. Scott, L. Radom. *J. Phys. Chem.*, **100**, 16502 (1996).
[20] P.R. Varadwaj, I. Cukrowski, H.M. Marques. *J. Phys. Chem.*, **112**, 10657 (2008).
[21] H. Chermette. *Coord. Chem. Rev.*, **178–180**, 699 (1998).
[22] L. Rulíšek, Z. Havlas. *J. Phys. Chem. A*, **103**, 1634 (1999).
[23] A. Ahmedova, P. Marinova, K. Paradowska, N. Stoyanov, I. Wawer, M. Mitewa. *Inorg. Chim. Acta*, **363**, 3919 (2010).
[24] Ş. Güveli, N. Özdemir, T. Bal-Demirci, B. Ülküseven, M. Dinçer, Ö. Andaç. *Polyhedron*, **29**, 2393 (2010).
[25] G. Bruno, M. Almeida, F. Artizzu, J.C. Dias, M.L. Mercuri, L. Pilia, C. Rovira, X. Ribas, A. Serpe, P. Deplano. *Dalton Trans.*, 4566 (2010).
[26] S. Naiyam, M.G.B. Drew, C. Estarellas, A. Frontera, A. Ghosh. *Inorg. Chim. Acta*, **363**, 3904 (2010).
[27] E. Stander-Grobler, O. Schuster, G. Heydenrych, S. Cronje, E. Tosh, M. Albrecht, G. Frenking, H.G. Raubenheimer. *Organometallics*, **29**, 5821 (2011).
[28] D.-P. Song, Y.-X. Wang, H.-L. Mu, B.-X. Li, Y.-S. Li. *Organometallics*, **30**, 925 (2011).
[29] J.G. Małecki, B. Machura, A. Świtlica. *Struct. Chem.*, **22**, 77 (2011).
[30] *SMART (Version 5.060) and SAINT (Version 6.02)*, Bruker AXS Inc., Madison, WI (1999).
[31] M.C. Burla, R. Caliandro, M. Camalli, B. Carrozzini, G.L. Cascarano, L. De Caro, C. Giacovazzo, G. Polidori, R. Spagna. *J. Appl. Cryst.*, **38**, 381 (2005).
[32] G.M. Sheldrick. *SHELXL97, Program for Crystal Structure Refinement*, University of Göttingen, Germany (1997).
[33] *SHELXT LN (Version 5.10)*, Bruker Analytical X-ray Inc., Madison, WI (1998).
[34] M.J. Frisch, G.W. Trucks, H.B. Schlegel, G.E. Scuseria, M.A. Robb, J.R. Cheeseman, G. Scalmani, V. Barone, B. Mennucci, G.A. Petersson, H. Nakatsuji, M. Caricato, X. Li, H.P. Hratchian, A.F. Izmaylov, J. Bloino, G. Zheng, J.L. Sonnenberg, M. Hada, M. Ehara, K. Toyota, R. Fukuda, J. Hasegawa, M. Ishida, T. Nakajima, Y. Honda, O. Kitao, H. Nakai, T. Vreven, J.A. Montgomery Jr., J.E. Peralta, F. Ogliaro, M. Bearpark, J.J. Heyd, E. Brothers, K.N. Kudin, V.N. Staroverov, R. Kobayashi, J. Normand, K. Raghavachari, A. Rendell, J.C. Burant, S.S. Iyengar, J. Tomasi, M. Cossi, N. Rega, J.M. Millam, M. Klene, J.E. Knox, J.B. Cross, V. Bakken, C. Adamo, J. Jaramillo, R. Gomperts, R.E. Stratmann, O. Yazyev, A.J. Austin, R. Cammi, C. Pomelli, J.W. Ochterski, R.L. Martin, K. Morokuma, V.G. Zakrzewski, G.A. Voth, P. Salvador, J.J. Dannenberg, S. Dapprich, A.D. Daniels, Ö. Farkas, J.B. Foresman, J.V. Ortiz, J. Cioslowski, D.J. Fox. Gaussian 09, Revision A.1, Gaussian, Inc., Wallingford, CT (2009).
[35] F. Valencia, A.H. Romero, M. Kiwi, R. Ramírez, A. Toro-Labbé. *Chem. Phys. Lett.*, **371**, 267 (2003).
[36] A. Vijayaraj, R. Prabu, R. Suresh, G. Jayanthi, J. Muthumary, V. Narayanan. *Synth. React. Inorg., Met.-Org., Nano-Met. Chem.*, **41**, 963 (2011).
[37] B. Türkkan, B. Sarıboğa, N. Sarıboğa. *Transition Met. Chem.*, **36**, 679 (2011).
[38] R. Takjoo, A. Akbari, M. Ahmadi, H. Amiri Rudbari, G. Bruno. *Polyhedron*, **55**, 225 (2013).
[39] M. Cocu, J. Gradinaru, M. Revenco, E. Rybak-Akimova, N. Gărbălău. *Chem. J. Moldova*, **3**, 38 (2008).
[40] J.I. Gradinaru, S.T. Malinovski, M.A. Popovici, M. Gdaniec. *Crystallogr. Rep.*, **50**, 217 (2005).
[41] (a) R. Takjoo, S.W. Ng, E.R.T. Tiekink. *Acta Crystallogr., Sect. E*, **68**, m911 (2012); (b) R. Takjoo, S.W. Ng, E.R.T. Tiekink. *Acta Crystallogr., Sect. E*, **68**, m944 (2012); (c) R. Takjoo, M. Ahmadi, A. Akbari, H. Amiri Rudbari, F. Nicolo. *J. Coord. Chem.*, **65**, 3403 (2012).
[42] Yu.A. Simonov, M.A. Yampolskaya, V.E. Zavodnik, V.M. Leovats, N.V. Gerbeleu, T.I. Malinovskii. *Zh. Neorg. Khim.*, **37**, 790 (1992).